

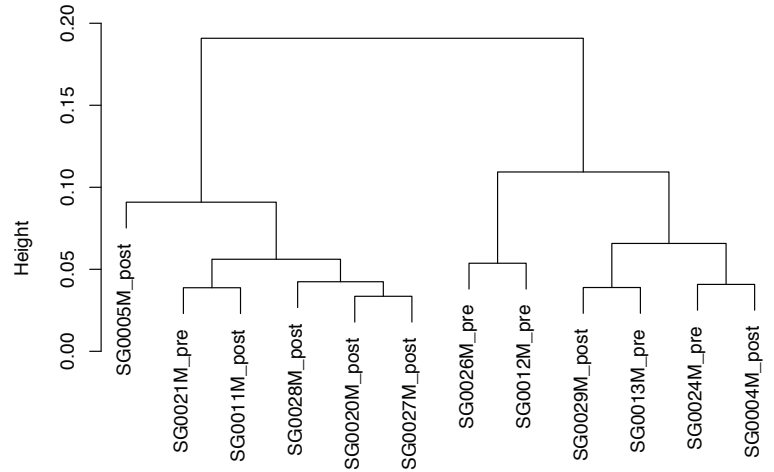
### Supplementary Figure S1

Analysis of TAMs density and phenotype post-NACT (A) Definiens analysis of human HGSOc omental metastases stained with anti-CD68 antibody. Left, TMA core from a single HGSOc biopsy sample from a patient who received NACT is shown. Centre, core overlaid with areas assigned as malignant cell islands (red) and as adjacent stroma (green). Right, core overlaid with areas assigned as positive CD68 staining (yellow), analysed within both tumor and stromal areas and darkly counterstained nuclei (blue). Scale bars, 200 $\mu$ m; 50 $\mu$ m in enlarged inserts. (B) Overall survival of nine HGSOc post-chemotherapy patients stratified by high (upper quartile) or low (lower quartile) CD68+ percentage area across whole tissue. (C) Overall survival of sixteen HGSOc pre-chemotherapy patients stratified by high (upper quartile) or low (lower quartile) CD68+ percentage area in the stromal area. (D) Gating strategy for human TAMs (E) Dot-plots with representative CD163 staining of human TAMs, with CD163+ gating, for three pre-NACT (left, red, orange and pink) and three post-NACT (right, green, blue and purple) samples. (F, G, H) Flow cytometry analysis of HGSOc omental metastases from nine patients treated with upfront surgery (green) and fourteen patients having received NACT (red). MFI calculated on median fluorescence for CD163, CD206 and HLA-DR staining of TAMs pre- and post-chemotherapy. Mann-Whitney test was applied.

**A**

		SG0012M_pre	SG0013M_pre	SG0021M_pre	SG0024M_pre	SG0026M_pre	SG0027M_post	SG0028M_post	SG0029M_post	SG0004M_post	SG0005M_post	SG0011M_post	SG0020M_post
Macrophage	CD14	8.89	9.81	9.48	8.93	9.51	9.05	8.88	9.23	9.47	8.71	9.32	9.59
	MARCO	8.17	8.46	4.34	5.06	2.87	7.09	6.53	6.35	6.90	3.97	7.07	7.07
	MSR1	8.97	8.84	7.17	7.42	8.77	7.33	7.56	8.05	8.79	4.71	6.92	7.33
	CD163	9.12	9.36	7.35	8.54	7.85	8.28	8.69	8.03	9.24	8.19	8.40	7.79
	EMP1	5.20	5.34	6.47	6.12	3.21	5.41	5.11	6.58	4.81	1.88	5.53	5.72
	CD68	-2.97	-1.97	-0.31	-2.57	-1.84	-1.88	-1.63	-0.54	-1.25	-0.79	-0.46	-0.74
Tcell	CD3E	ND	ND	ND	ND	ND	ND	ND	ND	ND	ND	ND	ND
	CD3G	ND	ND	ND	ND	ND	ND	ND	ND	ND	ND	ND	ND
	CD3D	-0.70	-2.15	-3.69	-3.91	-0.80	-1.69	-3.05	-2.49	-2.24	-3.46	-0.52	-3.86
	LCK	-0.79	-2.01	-4.03	-4.57	-1.33	-1.75	-4.75	-2.15	-2.79	-3.10	-0.77	-3.16
	LEF1	ND	ND	ND	ND	ND	ND	ND	ND	ND	ND	ND	ND
Bcell	CD19	ND	ND	ND	ND	ND	ND	ND	ND	ND	ND	ND	ND
	CR2	ND	ND	ND	ND	ND	ND	ND	ND	ND	ND	ND	ND
	TCL1A	ND	ND	ND	ND	ND	ND	ND	ND	ND	ND	ND	ND
	BACH2	-3.18	-1.84	-0.65	-1.61	-3.16	-2.26	-1.73	-1.96	-2.69	-2.06	-2.11	-0.91
Gr/cyte	MME	-2.95	-2.70	-1.82	-4.61	-5.71	-4.05	-1.20	-4.03	-4.40	-0.42	-0.67	-3.55
	IL8RA	ND	ND	ND	ND	ND	ND	ND	ND	ND	ND	ND	ND
	IL8RB	ND	ND	ND	ND	ND	ND	ND	ND	ND	ND	ND	ND
Mast	PRG2	ND	ND	ND	ND	ND	ND	ND	ND	ND	ND	ND	ND
	SIGLEC6	ND	ND	ND	ND	ND	ND	ND	ND	ND	ND	ND	ND
Epithel.	EPCAM	1.24	-4.70	-2.30	-0.50	2.80	-3.82	-2.56	-0.17	-0.68	-1.86	-5.19	-3.67
	PAX8	1.79	-0.82	-0.21	1.18	1.63	-0.87	-0.37	0.89	-0.16	-1.66	-0.17	-1.20
	WT1	1.75	-1.54	-1.85	-0.82	1.66	-2.16	-1.43	-1.17	-1.31	-2.01	-2.83	-2.50

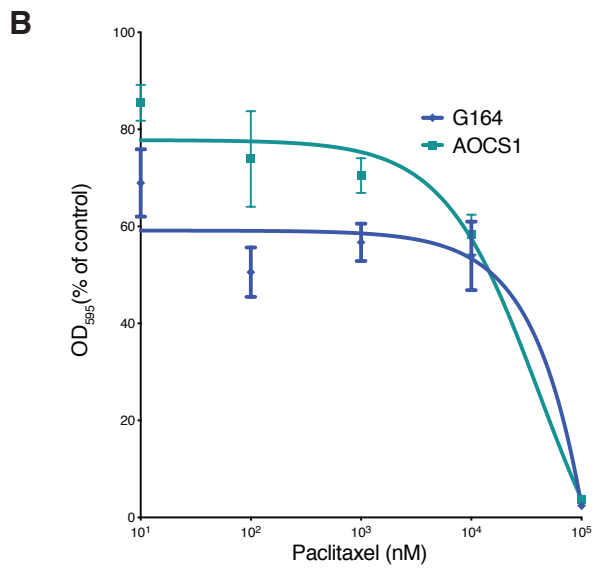
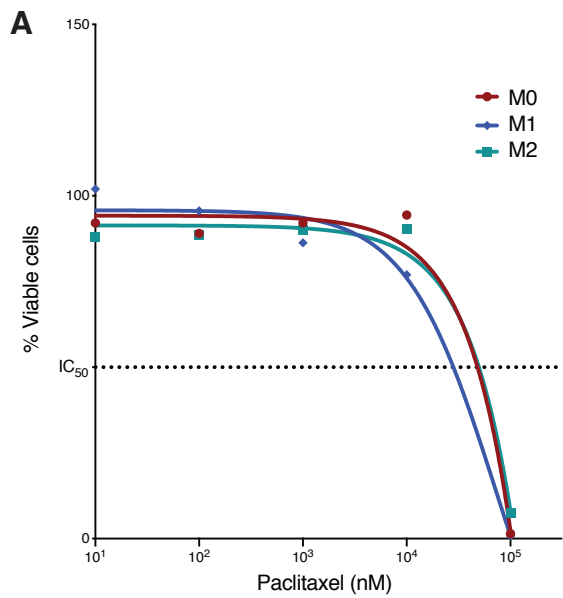
**B**



Supplementary Figure 2

### **Supplementary Figure S2**

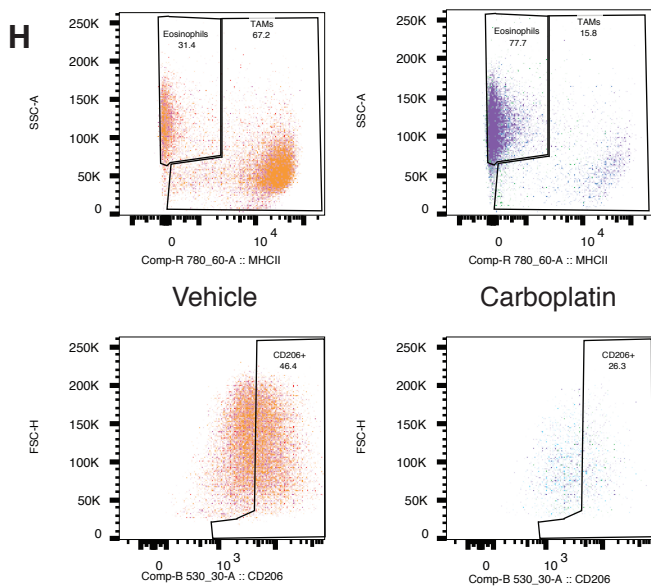
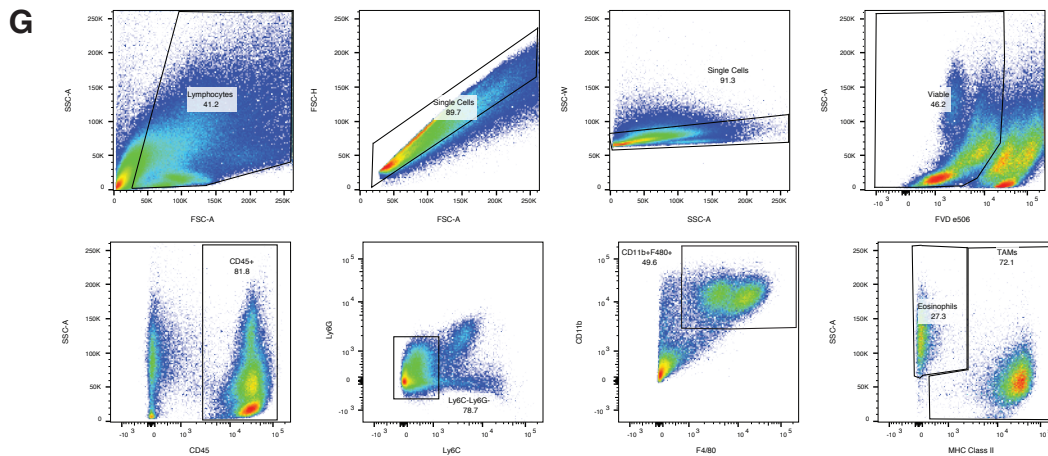
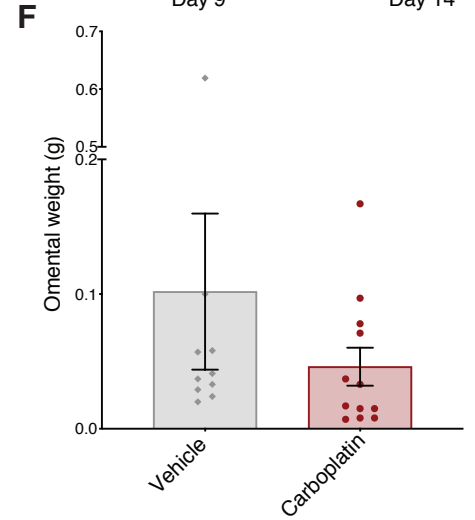
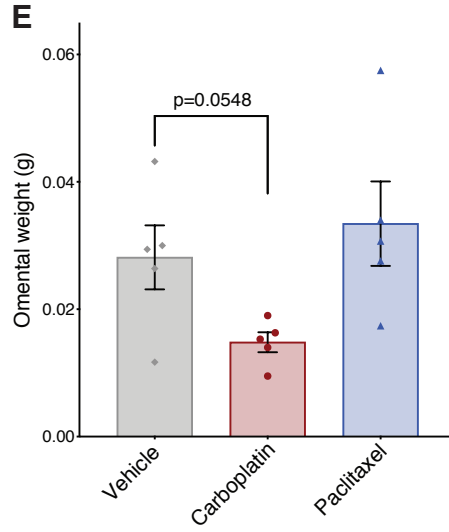
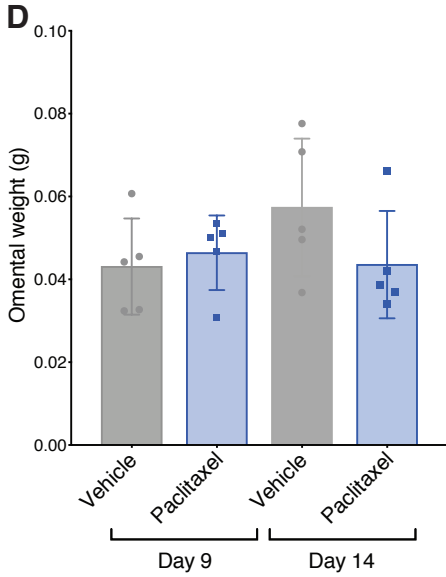
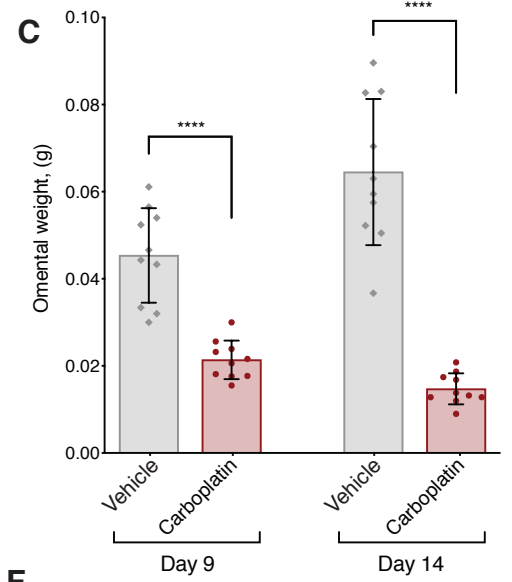
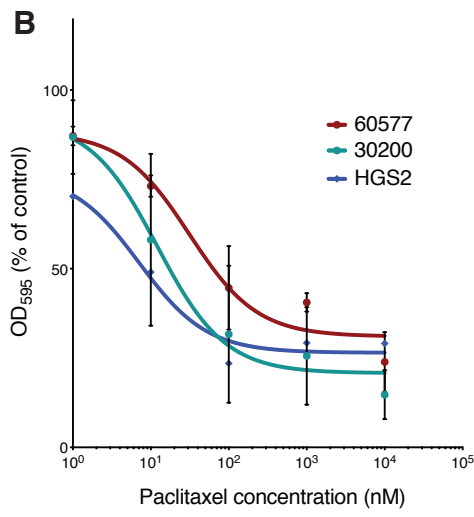
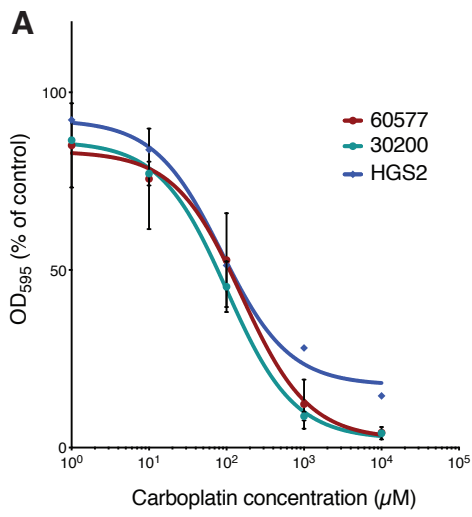
Purity and unsupervised clustering of TAM transcriptomes from pre- and post-chemotherapy biopsies (A) Log<sub>2</sub>RPKM gene expression of the indicated cell-type markers across all samples. Red to blue colour-spectrum corresponds to high to low values respectively. (B) Hierarchical cluster analysis of the samples based on Pearson's correlation matrix of all protein-coding genes.



Supplementary Figure 3

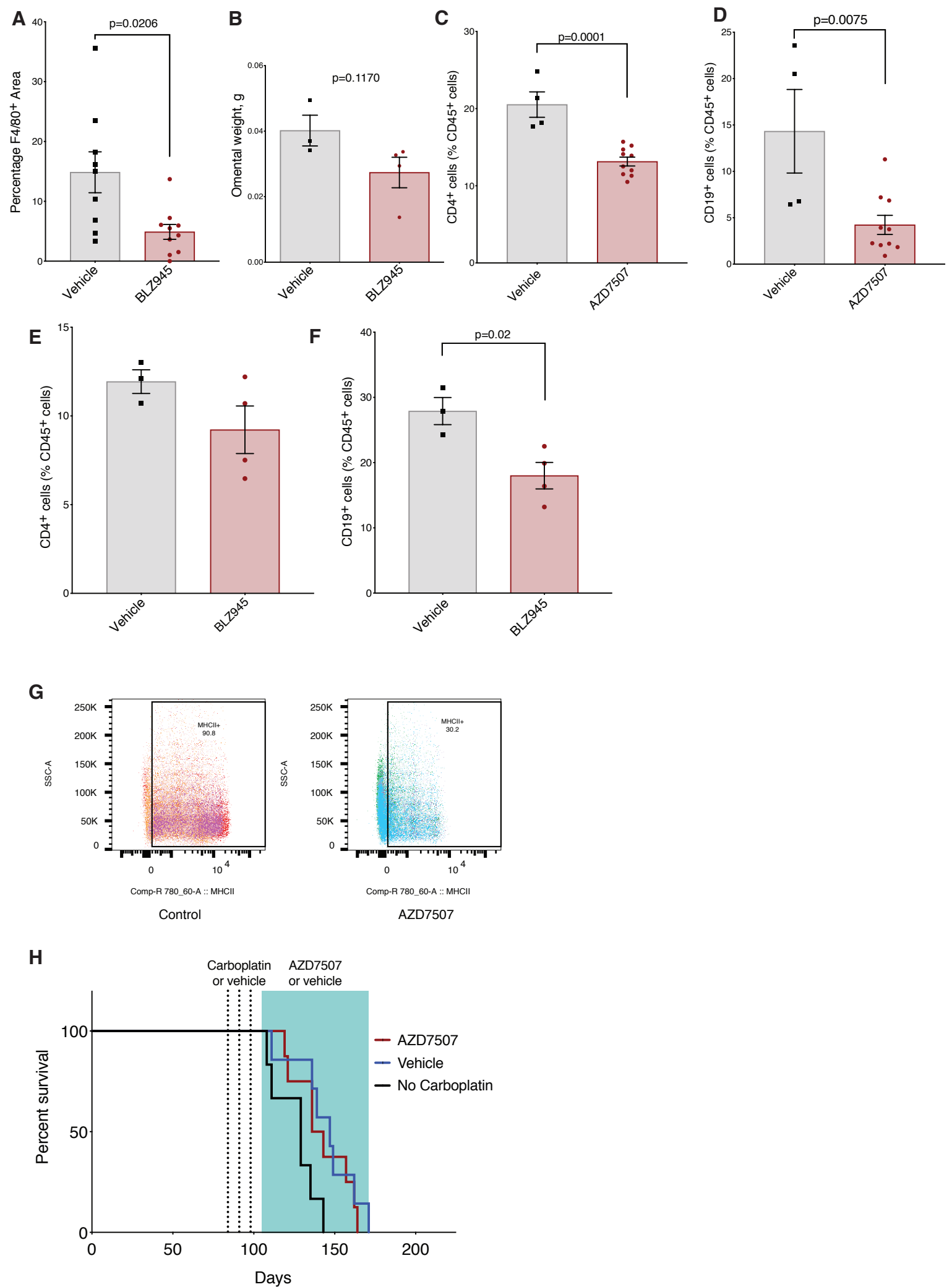
### Supplementary Figure S3

Sensitivity of macrophages and human HGSOc cell lines to paclitaxel (A) Human CD14<sup>+</sup> monocytes derived from leucocyte cones were differentiated in media containing h-MCSF for seven days prior to being polarised to M1 (blue line) and M2 (red line) phenotypes with LPS/IFN $\gamma$  and IL-4/IL-10 respectively, M0 (green line) cells received no additional stimulation. Cells were cultured in media containing varying concentrations of paclitaxel for 48 hours. Data represent viable cells expressed as the percentage of single cells, normalized to the media only control for each stimulation condition. Data relate to a single experiment. IC50 values: M0=  $7.72 \cdot 10^8$  nM, M1= $7.29 \cdot 10^4$  nM and M2= $7.77 \cdot 10^8$  nM. (B) AOCS1 (red line) and G164 (blue line) cells were cultured in media containing varying concentrations of paclitaxel for forty-eight hours. OD595 measurements for crystal violet staining presented as the mean with error bars representing SEM from three experiments, normalised to media-only control for paclitaxel. IC50 values: G164= $4.17 \cdot 10^6$ nM, AOCS1= $4.15 \cdot 10^4$ nM.

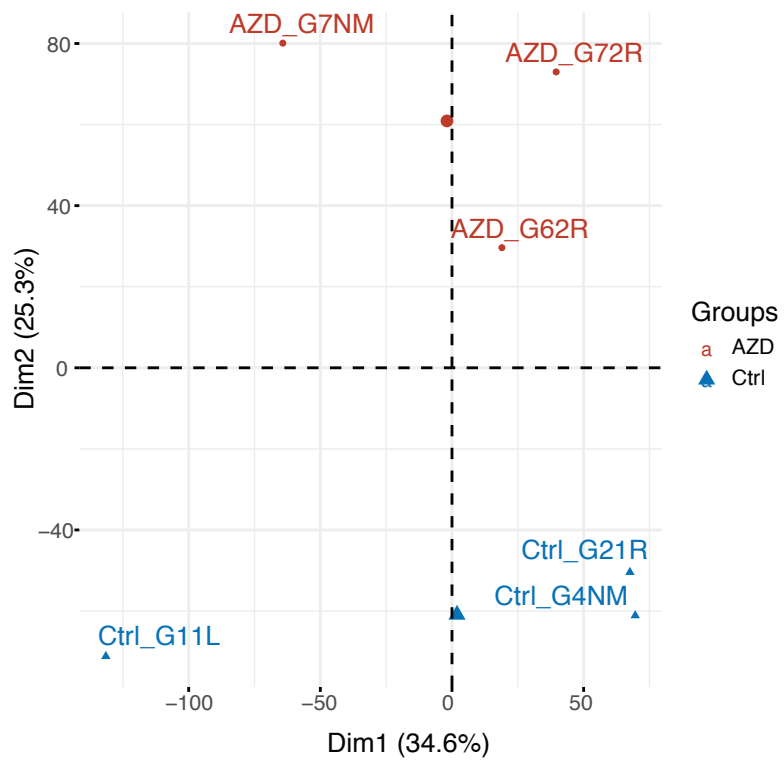


**Supplementary Figure S4** Response of HGSOC mouse cell lines to chemotherapy *in vitro* and *in vivo* (A, B) Effects of carboplatin (A) and paclitaxel (B) chemotherapy on the 60577 (red line), 30200 (green line) and HGS2 (blue line) cell lines *in vitro*. OD595 of crystal violet staining measurements presented as normalised to media-only control. 30200, 60577 and HGS2 data combined from three separate experiments. IC<sub>50</sub> values carboplatin: 60577=155µM, 30200=100µM HGS2=87µM; IC<sub>50</sub> paclitaxel 60577=31nM, 30200=12nM HGS2=7nM. (C, D, E, F) Omental tumor weight at the time-point analysed in Figure 4, (D-G) and 5 (A-H.) (C) Omental weight of 60577 tumors from mice culled at time points nine days and fourteen days of carboplatin treatment. Data relate to two experiments pooled together. (D) Omental weight of 60577 tumors from mice culled at time points nine days and fourteen days following of paclitaxel treatment. Data relate to a single experiment, five mice per group. (E) Omental weight of 30200 tumors treated with carboplatin, paclitaxel or vehicle from mice culled at a time point forty-eight hours following the last treatment. Data relates to a single experiment, five mice per group. (F) Omental HGS2 tumor weight recorded for mice culled 21 days after the first dose, following three doses. Data relate to two experiments, nine vehicle-treated mice and twelve carboplatin treated mice. (G) Gating strategy for TAMs in tumours from 60577 mouse model. (H) Dot-plots representing TAMs from 60577 model (top) and CD206 staining of TAMs (bottom). Each plot represents three mice from the experiment shown in figure 4D and 5A, 14 days time-point, treated with vehicle (left, red, orange and pink) or carboplatin (right, green, blue and purple).





**Supplementary Figure S5** Effect of TAM depletion in combination with chemotherapy (A) Quantification of F4/80 staining by Definiens analysis in relapsed 60577 tumors from the experiment shown in Figure 6I. F4/80 staining expressed as percentage positive area of the biopsy. (B) Effect of BLZ945 treatment started 21 days after 60577 cell injection and continued for 4 days on omental tumor weight. (C, D): Effect of AZD7507 treatment started 21 days after 60577 cell injection and continued for 12 days. Flow cytometry analysis of CD4<sup>+</sup> and CD19<sup>+</sup> cells as percentage of CD45. (E, F) Effect of BLZ945 treatment started 21 days after 60577 cell injection and continued for 4 days on omental tumor weight. Flow cytometry analysis of CD4<sup>+</sup> and CD19<sup>+</sup> cells as percentage of CD45. (G) Dot-plots representing TAMs from 60577 model stained for MHCII. Each plot represents three mice from the experiment shown in figure 6O , treated with control (left, red, orange and pink) or AZD7507 (right, green, blue and purple). (H) Kaplan Meier curves showing 30200 injected AZD7507 treated mice and vehicle-treated controls) when treatment is started seven days after carboplatin treatment. Carboplatin treatments are indicated (dashed lines), the period of AZD7507 or vehicle treatment is indicated (green shading). Data from a single experiment are shown.



Supplementary Figure 6

**Supplementary Figure S6** Clustering of AZD7507-treated ovarian mouse model tumors  
Unsupervised clustering of RNA-seq sample groups by principal-component analysis